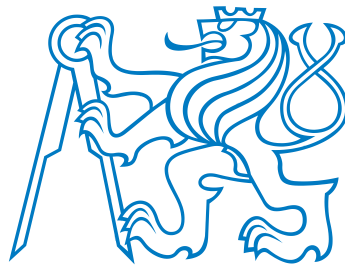


CZECH TECHNICAL UNIVERSITY IN PRAGUE

FACULTY OF CIVIL ENGINEERING

DEPARTMENT OF CONCRETE AND MASONRY STRUCTURES



DIPLOMA THESIS

Design of Concrete Structures Using Genetic Algorithm

Supervisor of the diploma thesis: doc. Ing. Petr Štemberk, Ph.D.

Prague, 2017

Bc. Jitka Mádlová

Declaration

I declare that I have written my diploma thesis myself and used only sources (literature, project, SW etc.) in enclosed bibliography.

In Prague _____

subscription

Acknowledgement

Foremost, I would like to thank to doc. Ing. Petr Štemberk, Ph.D. and Ing. Martin Petřík, Ph.D. for their excellent leadership, improving ideas and valuable advice. I would also like to express great gratitude to my family for their support, patience and calm study environment they provided.

Abstract

This diploma thesis deals with optimization of shapes of concrete structures. The shapes obtained from the developed algorithm can be used as inspiration for the designers of structures. Genetic Algorithm (GA) is used for the optimization process, when in each iteration, several structures are calculated and evaluated. The developed algorithm is inspired by Evolutionary Structural Optimization (ESO) that is based on removing inefficient material from the structure. The feature of adding material around the highly stressed places is also included in the algorithm. The structures are evaluated based on the distribution of the principal stresses. The displacements and the stresses are determined using the Finite Element Method (FEM). The whole optimization algorithm is implemented in MATLAB Environment. Examples of the structures obtained using the implemented algorithm are provided in this thesis.

Key words

Optimization, genetic algorithm (GA), evolutionary structural optimization (ESO), finite element method (FEM), architecture

Abstrakt

Tato diplomová práce se zabývá optimalizací tvaru betonových konstrukcí. Tvary, které jsou získány pomocí vytvořeného algoritmu, mohou být dále využity jako inspirace pro návrh konstrukcí. Optimalizační proces je vytvořený za použití Genetického Algoritmu (GA), v každé iteraci je vypočteno a vyhodnoceno několik konstrukcí. Vytvořený proces je inspirován metodou Optimalizace evolučních struktur (ESO), která je založená na odebírání nejméně využitého materiálu z konstrukce. V procesu je také zahrnuta funkce přidávání materiálu do velmi namáhaných míst. Konstrukce jsou ohodnoceny na základě hlavních napětí v konstrukci. Posuny a napětí jsou vypočteny metodou konečných prvků (MKP). Celý optimalizační proces je zpracován v prostředí MATLAB. Příklady konstrukcí získaných pomocí vytvořeného algoritmu jsou součástí práce.

Klíčová slova

Optimalizace, genetický algoritmus (GA), optimalizace evolučních struktur (ESO), metoda konečných prvků (MKP), architektura



ZADÁNÍ DIPLOMOVÉ PRÁCE

I. OSOBNÍ A STUDIJNÍ ÚDAJE

Příjmení: Mádlová	Jméno: Jitka	Osobní číslo: 395702
Zadávací katedra: Katedra betonových a zděných konstrukcí (K133)		
Studijní program: Stavební inženýrství		
Studijní obor: Konstrukce pozemních staveb		

II. ÚDAJE K DIPLOMOVÉ PRÁCI

Název diplomové práce: Navrhování betonových konstrukcí s využitím genetického algoritmu	
Název diplomové práce anglicky: Design of Concrete Structures Using Genetic Algorithm	
Pokyny pro vypracování:	
1) Vytvoření programu v prostředí MATLAB, který bude optimalizovat tvar konstrukce v závislosti na napětích. Program bude obsahovat vlastní výpočet metodou konečných prvků. Řešena bude dvourozměrná úloha.	
2) V práci bude teoreticky popsán genetický algoritmus a bude vysvětlen princip metody konečných prvků.	
Seznam doporučené literatury:	
J. Hynek. Genetické algoritmy a genetické programování.	
P.I. Kattan. MATLAB Guide to Finite Elements: An Interactive Approach.	
Jméno vedoucího diplomové práce: doc. Ing. Petr Štemberk , Ph.D.	
Datum zadání diplomové práce: 3. 10. 2016	Termín odevzdání diplomové práce: 8. 1. 2017
Údaj uveďte v souladu s datem v časovém plánu příslušného ak. roku	
Podpis vedoucího práce	Podpis vedoucího katedry

III. PŘEVZETÍ ZADÁNÍ

Beru na vědomí, že jsem povinen vypracovat diplomovou práci samostatně, bez cizí pomoci, s výjimkou poskytnutých konzultací. Seznam použité literatury, jiných pramenů a jmen konzultantů je nutné uvést v diplomové práci a při citování postupovat v souladu s metodickou příručkou ČVUT „Jak psát vysokoškolské závěrečné práce“ a metodickým pokynem ČVUT „O dodržování etických principů při přípravě vysokoškolských závěrečných prací“.

3. 10. 2016	
Datum převzetí zadání	Podpis studenta(ky)

Contents

1	Introduction	1
2	Two-Dimensional Stress and Strain	3
3	Finite Element Method	6
3.1	Four-node Quadrilateral Elements	6
3.2	Numerical Integration	8
4	Genetic Algorithm	11
4.1	Terminologies and Operators of GA	12
4.1.1	Population	12
4.1.2	Fitness Function	13
4.1.3	Selection and Reproduction	13
4.1.4	Genetic Operators	15
5	Evolutionary Structural Optimization	18
5.1	Structures Optimized Using ESO	19
5.2	Modified ESO Method	23
5.3	Strut-and-Tie Models	23
6	Optimization Using GA	25
6.1	Proposed Algorithm	25
7	Examples of Optimized Structures	33
7.1	Structure 1	33
7.2	Structure 2	39
7.3	Structure 3	44
8	Construction Aspects	49
9	Conclusions	51
	Bibliography	54
A	RFEM Results	I

List of Figures

1.1	The Aqueduct of Segovia, Spain	1
1.2	Office Building, Takatsuki, Japan, [18]	2
2.1	Two-dimensional State of Stress, Principal Stresses	3
2.2	Displacement and Rotations of Two-Dimensional Element	4
3.1	Finite Element Approximation for a One-Dimensional Case	6
3.2	Four-node Quadrilateral Element	7
3.3	Two-point Gaussian Quadrature in 1D	9
3.4	Four-point Gaussian Quadrature in 2D	9
4.1	Flowchart of GA	11
4.2	Representation of a Gene	13
4.3	Roulette Selection	14
4.4	Selection based on a) fitness, b) rank	15
4.5	Crossover operators. a) one-point, b) two-point, c) uniform, d) arithmetic	16
4.6	Mutation. a) bit inversion, b) adding a random value	17
5.1	Process of ESO	19
5.2	Example 1 - Design Domain	20
5.3	Example 1 - ESO Solutions	20
5.4	Example 2 - Design Domain	21
5.5	Example 2 - ESO Solutions	21
5.6	Example 3 - Design Domain	22
5.7	Example 3 - ESO Solutions	22
5.8	Example 3 - ESO Solutions	23
5.9	Example 2 - STM	24
6.1	Proposed Algorithm	26
6.2	Initial Model	27
6.3	Initial Population	27
6.4	Elements Kept	27
6.5	Mapping the Structure	28
6.6	Crossover	29

6.7	Mutation - Structure Extension	30
6.8	Mutation - Structure Reduction	30
6.9	Unconnected Elements	31
6.10	Disconnected Structure	31
6.11	Biaxial Strength of Concrete	32
6.12	Adding Material	32
7.1	Structure 1 - Design Domain	33
7.2	Structure 1 - The Evolution of Cost	34
7.3	Structure 1 - Distribution of Principal Stress σ_1	35
7.4	Structure 1 - Distribution of Principal Stress σ_2	36
7.5	Structure 1 - The Best Rated Structure	36
7.6	Structure 1 - The Evolution of Cost, 2nd Calculation	37
7.7	Structure 1 - Distribution of Principal Stress σ_1 , 2nd Calculation	37
7.8	Structure 2 - Design Domain	39
7.9	Structure 2 - The Evolution of Cost	39
7.10	Structure 2 - Distribution of Principal Stress σ_1	41
7.11	Structure 2 - Distribution of Principal Stress σ_2	42
7.12	Structure 2 - The Best Rated Structure	42
7.13	Structure 2 - Distribution of Principal Stress σ_2 , ESO	43
7.14	Structure 3 - Design Domain	44
7.15	Structure 3 - The Evolution of Cost	44
7.16	Structure 3 - Distribution of Principal Stress σ_1	46
7.17	Structure 3 - Distribution of Principal Stress σ_2	46
7.18	Structure 3 - The Best Rated Structure	47
7.19	Structure 3 - Resulting Structure	48
7.20	Structure 3 - Visualization	48
8.1	Prosta Tower, [4]	49
8.2	Warمیńska Shopping Gallery, [2], [15]	50
A.1	Loads	I
A.2	FE Mesh	I
A.3	Global Deformation u	II
A.4	Principal Stress Trajectories	II
A.5	Principal Stress σ_1	III

A.6 Principal Stress σ_2	III
---	-----

List of Tables

3.1	Locations and Weights in Gaussian Integration	10
4.1	Population	12
4.2	Selection	14
6.1	CEB-FIB Conditions	31
7.1	Structure 1 - Input Parameters	34
7.2	Structure 1 - Results	35
7.3	Structure 1 - Comparison of Calculations	38
7.4	Structure 2 - Input Parameters	40
7.5	Structure 2 - Results	41
7.6	Structure 3 - Input Parameters	45
7.7	Structure 3 - Results	45

Chapter 1

Introduction

In these days, ecological and environmental protection issues are often discussed. One of the related topics is material consumption which is closely connected to construction. The impact of construction on the environment is supposed to be reduced as much as possible. Therefore, an economical design is an important factor in the construction industry. From the perspective of material consumption, the total amount of materials in the structure should be utilized as much as possible.

It is well known, that the most beautiful structures carry its load efficiently. As a great example of these structures the Aqueduct of Segovia located in Spain was chosen. The Roman aqueduct, which was constructed probably during the 1st and the 2nd century AD, is shown in Fig. 1.1.

Figure 1.1: The Aqueduct of Segovia, Spain

Nowadays, the structures which have an origin in nature and its principles are found as the most remarkable and are often admired. The shapes of the structures can be also a result of some optimizing algorithm. Very suitable algorithm for optimizing the structures was found Evolutionary Structural Optimization (ESO), which is based on gradual removing inefficient material from a structure, [19]. The weight of the structure is being minimized, while the structure becoming more utilized. This method was already used for designing several structures such as office building in Takatsuki, Japan designed by Ohmori, shown in Fig. 1.2. The structure completed in April 2004 has two its walls optimized using Extended ESO. As follows from figures, the structure optimized using

this algorithm has also quite a remarkable shape. Results of ESO can be a great basis for architects designing new structures.

Figure 1.2: Office Building, Takatsuki, Japan, [18]

The aim of this diploma thesis is to develop the optimizing tool for engineers and architects. It was decided to combine the idea of ESO and Genetic Algorithm (GA), which is used especially for finding solutions to complex search problems. The goal is to obtain much more interesting shapes and let the user choose which solution or the part of the solution fits the best for his design.

The algorithms optimizing structures are closely connected to the Finite Element Method (FEM). The optimizing methods are removing the material from the structure based on the stress level, strain energy, or any other criterion specified for each finite element. Therefore, the FEM has to be implemented first, then deformations and stresses in the structure can be determined. The FEM solver, same as the whole optimization algorithm, is developed in MATLAB Environment.

The developed algorithm can be very useful for architects and engineers seeking inspiration for their future designing. The structures optimized by this tool should be moreover modified by an architect to get the shape that can be built. The construction of the structures with such an interesting shape is also quite challenging. In the end of this thesis, examples from the construction of unusually shaped structures are shown.

Chapter 2

Two-Dimensional Stress and Strain

The two-dimensional stress and strain which is important for the next calculations will be described in this chapter.

Two-dimensional state of stress is illustrated in Fig. 2.1. The element has sides dx and dy . Normal stresses σ_x and σ_y are acting in the x and y directions, while the shear stress τ_{xy} acts on the x edge in the y direction and the shear stress τ_{yx} acts on the y edge in the x direction.

Figure 2.1: Two-dimensional State of Stress, Principal Stresses

The shear stress τ_{xy} is equal to τ_{yx} , [12]. Therefore it is possible to write down three independent stresses as

$$\sigma = \begin{Bmatrix} \sigma_x \\ \sigma_y \\ \tau_{xy} \end{Bmatrix}. \quad (2.1)$$

Maximum and minimum normal stresses called principal stresses can be written for two-dimensional plane as

$$\sigma_1 = \frac{\sigma_x + \sigma_y}{2} + \sqrt{\left(\frac{\sigma_x - \sigma_y}{2}\right)^2 + \tau_{xy}^2} = \sigma_{max}, \quad (2.2)$$

$$\sigma_2 = \frac{\sigma_x + \sigma_y}{2} - \sqrt{\left(\frac{\sigma_x - \sigma_y}{2}\right)^2 + \tau_{xy}^2} = \sigma_{min}. \quad (2.3)$$

The principal angle is explained in Fig. 2.1 and is defined by

$$\tan 2\theta_p = \frac{2\tau_{xy}}{\sigma_x - \sigma_y}. \quad (2.4)$$

Displacement and rotations of two-dimensional element are illustrated in Fig.2.2.

Figure 2.2: Displacement and Rotations of Two-Dimensional Element

Equations describing the relationships between strains and displacements are given as

$$\varepsilon_x = \frac{\partial u}{\partial x}, \quad \varepsilon_y = \frac{\partial v}{\partial y}, \quad \gamma_{xy} = \frac{\partial u}{\partial y} + \frac{\partial v}{\partial x}, \quad (2.5)$$

where ε_x , ε_y are normal strains and γ_{xy} is shear strain. The vector representing strains could be written as

$$\{\varepsilon\} = \begin{Bmatrix} \varepsilon_x \\ \varepsilon_y \\ \gamma_{xy} \end{Bmatrix}. \quad (2.6)$$

There are two important concepts known as plane stress and plane strain. For both concepts, the stress-strain relationship for isotropic materials will be described.

Plane Stress

For the plane stress are following stresses equal to zero,

$$\sigma_z = \tau_{xz} = \tau_{yz} = 0. \quad (2.7)$$

The shear strains γ_{xz} , γ_{yz} are equal to zero, but ε_z differ from zero. The constitutive matrix for plane stress is given as

$$[D] = \frac{E}{1-\nu^2} \begin{bmatrix} 1 & \nu & 0 \\ \nu & 1 & 0 \\ 0 & 0 & \frac{1-\nu}{2} \end{bmatrix}, \quad (2.8)$$

where E is the modulus of elasticity, and ν is Poisson's ratio.

Plane Strain

For the plane strain are following strains equal to zero,

$$\varepsilon_x = \gamma_{xz} = \gamma_{yz} = 0. \quad (2.9)$$

The shear stresses τ_{xz} , τ_{yz} are equal to zero, but σ_z differ from zero. The constitutive matrix for plane strain is given as

$$[D] = \frac{E}{(1 + \nu)(1 - 2\nu)} \begin{bmatrix} 1 - \nu & \nu & 0 \\ \nu & 1 - \nu & 0 \\ 0 & 0 & \frac{1-2\nu}{2} \end{bmatrix}, \quad (2.10)$$

where E is the modulus of elasticity, and ν is Poisson's ratio.

The general linear relation between stress and strain vector well-known as generalized Hook's law has the following form

$$\{\sigma\} = [D]\{\varepsilon\}, \quad (2.11)$$

where $\{\sigma\}$ is the stress vector, $[D]$ is the constitutive matrix and $\{\varepsilon\}$ is the strain vector.

Chapter 3

Finite Element Method

The Finite Element Method (FEM) is applied to solve problems in many various fields of science. This thesis is focused on the stress analysis and its solving using FEM. But also the thermal analysis, fluid flow analysis, piezoelectric analysis, and many others are daily solved by this unique method. The FEM gives us a prediction of the behavior of systems, which is used by engineers and scientists for design and performance analyses.

In these days, a wide selection of commercial finite element analysis programs, which are able to calculate stress analysis, is provided. In this thesis, the solver of the stress analysis is implemented as a part of the developed algorithm in MATLAB Environment.

The FEM is a numerical method which seeks an approximate solution of the distribution of field variables in the problem domain. The field variables can be the displacement in stress analysis, the temperature or heat flux in thermal analysis, the electrical charge in electrical analysis, etc. The problem domain is divided into several elements with the physical laws applied to each element. Finite element approximation for a one-dimensional case is shown in Fig 3.1.

Figure 3.1: Finite Element Approximation for a One-Dimensional Case

3.1 Four-node Quadrilateral Elements

The stress analysis is solved using two-dimensional isoparametric finite elements with linear shape functions in the x and y directions. These elements are suitable for plane stress and plane strain problems. Four-node Quadrilateral Element has defined modulus

of elasticity E , Poisson's ratio ν , and thickness t . From its name is clear, that element has four nodes with two degrees of freedom at each node. The element is shown in Fig. 3.2. The basic feature of an isoparametric element is mapping the physical coordinates by the same shape functions which are used for approximation. The shape functions have the following form

$$\begin{aligned} N_1 &= \frac{1}{4} (1 - \xi)(1 - \eta), \\ N_2 &= \frac{1}{4} (1 + \xi)(1 - \eta), \\ N_3 &= \frac{1}{4} (1 + \xi)(1 + \eta), \\ N_4 &= \frac{1}{4} (1 - \xi)(1 + \eta), \end{aligned} \quad (3.1)$$

where ξ and η are nodal coordinates. Element with natural coordinates is shown in Fig. 3.2. This figure displays mapping from the Natural to the physical Cartesian coordinate system.

Figure 3.2: Four-node Quadrilateral Element

The formulation of the element stiffness matrix for the four-node quadrilateral element is given as

$$[K^e] = \int_{\Omega} [B]^T [D] [B] d\Omega = t \int_{-1}^1 \int_{-1}^1 [B]^T [D] [B] [J] d\xi d\eta, \quad (3.2)$$

where t is a thickness of the element, $[D]$ is the constitutive matrix for the plane stress/strain and $[J]$ is Jacobian matrix and $[B]$ are the derivatives of shape functions. Jacobian matrix has the following formulation

$$[J] = \begin{bmatrix} \frac{\partial N_1}{\partial \xi} & \frac{\partial N_2}{\partial \xi} & \frac{\partial N_3}{\partial \xi} & \frac{\partial N_4}{\partial \xi} \\ \frac{\partial N_1}{\partial \eta} & \frac{\partial N_2}{\partial \eta} & \frac{\partial N_3}{\partial \eta} & \frac{\partial N_4}{\partial \eta} \end{bmatrix} \begin{bmatrix} x_1 & y_1 \\ x_2 & y_2 \\ x_3 & y_3 \\ x_4 & y_4 \end{bmatrix}, \quad (3.3)$$

and $[B]$ matrix can be written as

$$[B] = \begin{bmatrix} \frac{\partial N_1}{\partial x} & 0 & \frac{\partial N_2}{\partial x} & 0 & \frac{\partial N_3}{\partial x} & 0 & \frac{\partial N_4}{\partial x} & 0 \\ 0 & \frac{\partial N_1}{\partial y} & 0 & \frac{\partial N_2}{\partial y} & 0 & \frac{\partial N_3}{\partial y} & 0 & \frac{\partial N_4}{\partial y} \\ \frac{\partial N_1}{\partial y} & \frac{\partial N_1}{\partial x} & \frac{\partial N_2}{\partial y} & \frac{\partial N_2}{\partial x} & \frac{\partial N_3}{\partial y} & \frac{\partial N_3}{\partial x} & \frac{\partial N_4}{\partial y} & \frac{\partial N_4}{\partial x} \end{bmatrix}. \quad (3.4)$$

The element external force vector is given as

$$\{f^e\} = \{f_\Omega^e\} + \{f_\Gamma^e\}, \quad (3.5)$$

where $\{f_\Omega^e\}$ and $\{f_\Gamma^e\}$ are the body and the boundary force vectors, which could be written in the following form

$$\{f_\Omega^e\} = \int_{\Omega} [N]^T \bar{X} d\Omega, \quad (3.6)$$

$$\{f_\Gamma^e\} = \int_{\Gamma_p^e} [N]^T \bar{p} d\Gamma. \quad (3.7)$$

$[N]$ is the vector of shape functions, \bar{X} is the vector of body forces and \bar{p} is the vector of distributed surface forces. Γ_p^e is the portion of the element boundary where the distributed surface load is applied.

When the global matrix $[K]$ and the global nodal force vector $\{f\}$ are obtained, the Eq. 3.8 for the structure is solved. As a result, the global nodal displacement vector $\{u\}$ is obtained,

$$[K]\{u\} = \{f\}. \quad (3.8)$$

When the displacements are calculated, the stress vector for each element is found as

$$\{\sigma^e\} = [D][B]\{u^e\}, \quad (3.9)$$

where $\{u^e\}$ is the element displacement vector.

3.2 Numerical Integration

The formulation of the element stiffness matrix given in Eq. 3.2 still needs to be integrated. Due to the complexity of the expression, the integration is usually done numerically. There are several methods which can be used for the numerical evaluation of definite integrals, [12]. In this thesis, Gauss quadrature method which was found the most useful in finite element applications is described, [14].

Figure 3.3: Two-point Gaussian Quadrature in 1D

Gauss quadrature method is illustrated graphically for the one-dimensional case in Fig. 3.3. In order to evaluate the integral, the function is evaluated at several sampling points. Each value f_i is multiplied by an appropriate weight w_i , and added. The quadrature formula for the one-dimensional case is given in Eq. 3.10. The sampling points are chosen in order to achieve the best possible accuracy. The location of sampling points is symmetrical about the center of the interval. The weight value is the same for symmetrically located points.

$$I = \int_{-1}^1 f(\xi) d\xi \simeq \sum_{i=1}^n w_i f_i = \sum_{i=1}^n w_i f_i(\xi_i) \quad (3.10)$$

The quadrature formula for the two-dimensional case can be written as

$$\begin{aligned} I &= \int_{-1}^1 \int_{-1}^1 f(\xi, \eta) d\xi d\eta = \int_{-1}^1 \left[\sum_{i=1}^n w_i f(\xi_i, \eta) \right] d\eta \\ &= \sum_{j=1}^n w_j \left[\sum_{i=1}^n w_i f(\xi_i, \eta_j) \right] = \sum_{i=1}^n \sum_{j=1}^n w_i w_j f(\xi_i, \eta_j), \end{aligned} \quad (3.11)$$

where w_i is the weight associated with the i -th point, and n is the number of sampling points. Table 3.1 gives the locations and weights of Gauss points up to four points.

Figure 3.4: Four-point Gaussian Quadrature in 2D

Table 3.1: Locations and Weights in Gaussian Integration

Number of Points, n	Location, ξ_i	Weight, w_i
1	$\xi_1 = 0.00000\ 00000\ 00000$	2.00000 00000 00000
2	$\xi_1, \xi_2 = \pm 0.57735\ 02691\ 89626$	1.00000 00000 00000
3	$\xi_1, \xi_3 = \pm 0.77459\ 66692\ 41483$	0.55555 55555 55555
	$\xi_2 = 0.00000\ 00000\ 00000$	0.88888 88888 88888
4	$\xi_1, \xi_4 = \pm 0.86113\ 63115\ 94053$	0.34785 48451 47454
	$\xi_2, \xi_3 = \pm 0.33998\ 10435\ 84856$	0.65214 51548 62546

Chapter 4

Genetic Algorithm

Genetic Algorithm (GA) is inspired by natural evolution and uses genetics as a model to find solutions to complex problems. The history of GA dates back to 1975, when it was introduced by John Holland in his book "Adaptation in natural and artificial systems". It is a heuristic method which is used as a tool for optimization problems which are difficult to solve using analytical methods. In these days, Genetic Algorithms found numerous applications in many fields. The process of GA is illustrated in the Fig. 4.1.

Figure 4.1: Flowchart of GA

GA is an iteration process which works with a set of individuals called population, where every individual is a unique solution to the given problem. The initial population can be generated randomly. It is appropriate that the initial population is large enough and it consists of a wide diversity of individuals. For the functioning of the whole algorithm, the proper fitness function has to be defined. In each iteration, individuals are selected for reproduction according to the fitness function. The better-rated individuals have a greater chance for reproduction than individuals with bad evaluation. In the next step, offspring are reproduced from the selected individuals using the crossover (recombination) and mutation. After that, the new individuals are evaluated by fitness function and replace the previous population. When the population converges to the optimal solution or the maximum iteration is reached, the process is stopped.

4.1 Terminologies and Operators of GA

4.1.1 Population

Individuals can be expressed in terms of the model as phenotype or in terms of GA like genotype. The mapping between phenotype and genotype is a very important step that provides functioning of the whole process. The solutions from the model are converted into chromosomes that the GA can work with, or, conversely. Generally, the genotype is characterized by only one chromosome. Each chromosome is subdivided into several genes which correspond to each factor in the solution. In case of binary representation, each gene consists of a bit string initialized to zero or one. The example of the population consisting of four chromosomes is shown in the Tab. 4.1 below.

Table 4.1: Population

Individual no.	Chromosome
1	1 1 1 0 0 1 1
2	0 1 1 1 1 0 1 1
3	0 0 0 1 0 0 0 1
4	1 1 0 0 1 1 0 0

The chromosome no. 1 from the Tab. 4.1 can be divided into genes as is shown in the following Fig. 4.2.

Figure 4.2: Representation of a Gene

4.1.2 Fitness Function

Each decoded chromosome is evaluated according to the fitness function. The fitness of individual indicates how good or conversely bad the solution is. The higher fitness, the better solution. It can be hard to define the fitness function for problem consisting more criteria. Choice of right fitness function affects the whole process. The selection could be also processed using cost function based on the principle the lower, the better.

4.1.3 Selection and Reproduction

In the next step, the evaluated chromosomes need to be selected into pairs for crossing. It is important to find good individuals from the population that will create offspring for the next generation. Another task is how many offspring each individual create. The individuals with better evaluation have more chance to be selected. The percentage of chance that individuals will create offspring is given by the selection pressure. High selection pressure indicates that very small number of individuals is selected for reproduction. In some cases, the very high selection rate can cause diversity loss of the population and the population could converge to a local minimum of a search space. On the other hand, the very low selection rate implies very long time to find an optimal solution. Therefore, it is recommended to keep a good balance between selection rate and other factors influencing the diversity of the population, such as crossover and mutation.

Selection schemes can be divided into proportionate-based selection and ordinary-based selection.

In the case of proportionate-based selection, the individuals are selected according to their fitness values relatively to the fitness of the other individuals in the population. The probability p_i that an individual i makes copy of its genome is given as

$$p_i = \frac{f_i}{\sum_{j=1}^N f_j} \quad i \in \{1, \dots, N\}, \quad (4.1)$$

where f_i is the fitness value of i -th individual and N is the size of the population. It is assuming, that fitness function is non-negative.

Ordinary-based selection means that individuals are selected based on their rank within the population. It means that in this case the selection pressure is not based on fitness distribution within the population.

Roulette Wheel Selection

Figure 4.3: Roulette Selection

Roulette Selection is one of the GA proportionate-based selection techniques. It is illustrated in the Fig. 4.3, where the roulette is divided into several slots which correspond to individuals. The size of slots is proportional to the reproduction probabilities p_i of individuals. The selection is based on spinning the wheel until the number of individuals in population N is reached. After each spin, the individual corresponding to the slot, where the ball remained, is selected to be a parent for the next generation.

In Tab. 4.2 are shown the individuals corresponding to the roulette wheel in Fig. 4.3.

Table 4.2: Selection

Individual no.	Chromosome	Fitness f_i	Probability p_i	Cumulative Probability
1	1 1 1 0 0 0 1 1	4	20 %	0.2
2	0 1 1 1 1 0 1 1	8	40 %	0.6
3	0 0 0 1 0 0 0 1	2	10 %	0.7
4	1 1 0 0 1 1 0 0	6	30 %	1.0

It is clear, that individual no. 2 has better chance to reproduce than individual no. 3. But the chance of reproduction is random, so it is possible that the badly ranked individual will reproduce. During each selection, a random number r between 0 and 1 is chosen and the i -th individual is selected according to the followed expression

$$\sum_{j=1}^{i-1} p_j < r \leq \sum_{j=1}^i p_j \quad i \in \{1, \dots, N\}, \quad (4.2)$$

where N is the size of the population and p is the reproduction probability.

Rank Selection

Rank Selection is ordinary-based selection technique. When the fitness of individuals differs very much, the Rank Selection is more suitable than the previous selection method. As the name implies, the selection is based on the rank of the individuals. Every chromosome receives fitness based on its rank, then for the population with N chromosomes the best chromosome has fitness N and the worst has fitness 1. The Fig. 4.4 shows the difference between selection based on fitness and based on rank for the same population.

Figure 4.4: Selection based on a) fitness, b) rank

There are also different types of selection such as Random Selection and Tournament Selection which are clearly explained in [16].

Elitism

In the case of improving the GA's performance, the best n individuals are copied to the new population. The rest of the process is done in its casual way.

4.1.4 Genetic Operators

Genetic operators bring diversity to the population and help GA converges to the optimal solution.

Crossover

Crossover is an important source of evolution which contain a process of producing new offspring. When the selection process is finished and the suitable individuals are prepared, crossover operator can be used for mating. The right choice of the operator brings better offspring which means better solutions for the problem. Crossover operators are divided into various types, some of them are displayed in Fig. 4.5.

Figure 4.5: Crossover operators. a) one-point, b) two-point, c) uniform, d) arithmetic

One-point crossover

One-point crossover is suitable for discrete or real value representations. The crossover point is selected randomly for both mated individuals and their content is exchanged around the point.

Two-point crossover

The principle is the same as for One-point crossover, except that the two crossover points are randomly selected.

Multi-point crossover

The number of crossover points is random and content between these points is exchanged.

Uniform crossover

Uniform crossover fits for real value representations. The content is randomly changed at n random positions.

Arithmetic crossover

Arithmetic crossover fits also for real value representations. It performs some kind of arithmetic operation to create new offspring.

Mutation

The mutation prevents the algorithm to end up in a local minimum and also helps maintain diversity in the population. One or more positions of the chromosome are changed according to the set mutation probability p_m . The appropriate value of mutation probability is chosen due to the problem solved. The mutation has also various types, such as bit inversion or adding a random value to a position in real value representations, shown in Fig. 4.6.

Figure 4.6: Mutation. a) bit inversion, b) adding a random value

Chapter 5

Evolutionary Structural Optimization

In this thesis, the concept of evolutionary structural optimization (ESO) is used. This concept helps to create the first population which is an input for the next optimization with GA, Chapter 6. The output from ESO is satisfying for the simple structures, but for the purposes of more complex problems, more evolution algorithms are combined together.

The concept of ESO is based on slowly removing inefficient material from a structure when the shape of the structure develops towards an optimum residual shape. At first, the structure is divided into small finite elements which are representing the material of the structure. The finite elements are gradually removed from the finite element model based on the stress level of each element.

It is possible to measure the stress level using some sort of average of all the stress components. One of the most used criteria for isotropic materials is the von Mises stress σ_v . Its formulation for the plane stress problems can be written as

$$\sigma_v = \sqrt{\sigma_x^2 + \sigma_y^2 - \sigma_x\sigma_y + 3\tau_{xy}^2}, \quad (5.1)$$

where σ_x and σ_y are normal stresses in x and y directions and τ_{xy} is the shear stress. More information about plane stress is written in Chapter 2. The comparison of the von Mises stress of the element σ_v to the maximum von Mises stress of the whole structure $\sigma_{v,max}$ gives as formulation for the stress level

$$\frac{\sigma_{v,e}}{\sigma_{v,max}} < RR_i, \quad (5.2)$$

where RR_i is the current rejection ratio. All the finite elements which satisfy this criterion are removed from the finite element model. The removal is repeated for the whole cycle of finite element analysis. The value RR_i is held until no more elements being removed at the present iteration. This is called steady-state. After reaching steady-state an evolutionary rate ER is added to rejection ratio. It can be defined as

$$RR_{i+1} = RR_i + ER \quad i = 0, 1, 2, 3, \dots, \quad (5.3)$$

The increased rejection ratio is held until reaching new steady-state. The evolutionary process takes place until the ending criterion is reached. For example, the ending criterion

occurs, when stress levels for all finite elements are higher than 25 % of the maximum, [19]. Typical values of initial rejection RR_0 and evolutionary rate ER are 1 %, but for some cases a much lower values could be needed.

Figure 5.1: Process of ESO

5.1 Structures Optimized Using ESO

The described method of ESO was implemented by author of this thesis in MATLAB Environment. The Flowchart of the process is shown in Fig. 5.1. In this subsection are shown structures which were optimized by this algorithm. All structures are divided into rectangular elements with eight degrees of freedom.

Example 1

Figure 5.2: Example 1 - Design Domain

The first example of the optimized structure is a domain of the size 2 x 4 m ($H \times L$) and thickness 0.1 m with two fixed supports. The vertical load F equal to 10 kN is acting in the middle of the span on the bottom side according to Fig. 5.2. Young's modulus $E = 33$ GPa and Poisson's ratio $\nu = 0.2$ are given. The problem is solved as symmetric. The half of the structure is divided into 900 elements. The initial rejection ratio RR_0 and evolutionary rate ER are both set to 1 %. The following Fig. 5.3 shows the shapes of the structure during iterations of ESO.

Figure 5.3: Example 1 - ESO Solutions

Example 2

Figure 5.4: Example 2 - Design Domain

The structure of the size 2 x 6 m ($H \times L$) and thickness 0.1 m with two roller supports was solved. The problem was calculated symmetric, same as the previous example. The horizontal move is restricted due to vertical symmetry in the middle of the span. The vertical load F equal to 10 kN is acting in the middle of the span on the top side according to Fig. 5.4. Young's modulus $E = 33$ GPa and Poisson's ratio $\nu = 0.2$ are given. The half of the structure is divided into 600 elements. RR_0 and ER are both set to 1 %. The shapes of the structure in iteration 1, 25, 50 and 75 are shown in Fig. 5.5.

Figure 5.5: Example 2 - ESO Solutions

Example 3

Figure 5.6: Example 3 - Design Domain

The third example shows the structure of size 2 x 10 m ($H \times L$) and thickness 0.1 m with two roller supports. The problem was calculated symmetric, same as the previous examples. The distributed load f equal to 10 kN/m is acting on the top side of the structure. This example has two different cases according to the location of supports. The supports are placed in the bottom corners or in the top corners of the structure. Both cases are illustrated in Fig. 5.6. Young's modulus $E = 33$ GPa and Poisson's ratio $\nu = 0.2$ are given. The half of the structure is divided into 1000 elements. For both cases, RR_0 is set to 1 % and ER is set to 0.1 %.

The shapes of the structures with supports in the bottom corners in iteration 1, 50, 150 and 200 are shown in the Fig. 5.7.

Figure 5.7: Example 3 - ESO Solutions

The shapes of the structures with supports in the top corners in iteration 1, 50, 150 and 250 are shown in the Fig. 5.8.

Figure 5.8: Example 3 - ESO Solutions

5.2 Modified ESO Method

The ESO is used for finding the optimal shape of the structure where the material is utilized as much as possible. Originally, the von Mises stress is used for the measuring the stress in the structure. But this criterion is not suitable for the concrete structures, because it does not distinguish between tension and compression areas in the structure. The criterion can be modified and the stress level for the compression dominant structures is then written as

$$\sigma_e = -\sigma_1 - \sigma_2, \quad (5.4)$$

where σ_1 and σ_2 are the maximum and the minimum principal stresses. At first, the elements where the tension dominates are removed. The tensile dominant structure is obtained using the modified criterion,

$$\sigma_e = \sigma_1 + \sigma_2. \quad (5.5)$$

In this case, the compression dominant elements are removed at first place, [17].

5.3 Strut-and-Tie Models

It is worth mentioning that the ESO can be also used as an efficient tool to determine the optimal strut-and-tie models (STM) for reinforced concrete structures, [1] and [10]. In this method, the reinforced concrete structure is transferred to compression struts and tension ties, while struts represent concrete and ties represent steel. The STM are mainly used for the design of distributed regions in concrete structures such as corbels, deep beams, beams with opening and piers. The inefficient material is removed based on the von Mises stress criterion.

The structure from the Example 2 shown in Fig. 5.5 is a great example of this technique. The structure obtained from iteration 75 can be also displayed as follows.

Figure 5.9: Example 2 - STM

In Fig. 5.9, the regions in red and blue respectively indicate the compressed and tensioned regions.

Chapter 6

Optimization Using GA

In this chapter, the algorithm implemented in MATLAB Environment is described. The results of ESO obtained in Chapter 5 are satisfying. The method works fine for the simple structures with appropriate input of rejection ratio RR and evolutionary rate ER . Appropriate rates for simple structures with a smaller number of elements are found easily. Finding appropriate rates become difficult with the increasing complexity of the structure and a growing number of elements. The structure loses its effectivity when a large number of elements are removed in one step. Therefore, methods that also enable adding material to the highly stressed regions in the structure were invented. These methods are based on ESO, such as Extended ESO and Bi-directional ESO, [3] and [13]. The feature of adding material is also included in implemented algorithm. The elements are added to regions where the stresses exceed the maximum capacity. The process of reducing elements according to stresses is implemented as a part of GA. The population is composed of chromosomes representing calculated structures. The structures are combined during the process with hope to go through the whole search space and find also the solution which would be probably skipped in ESO. The flowchart of proposed algorithm is shown in Fig. 6.1.

6.1 Proposed Algorithm

Each step of proposed algorithm in Fig. 6.1 will be described more detailed using following illustrative example. The example is a structure with two fixed supports loaded in the middle of the span.

Input Parameters

At first, the input parameters such as material parameters, initial geometry of the structure, loads, supports, mesh size and the parameters of GA are inserted. The GA parameters are number of chromosomes, number of iterations, elitism rate and probability of mutations. When the applied load and the supports are placed symmetric, it is possible to apply the symmetry boundary conditions as is shown in Fig. 6.2. The calculation with half number of elements is obviously shorter.

Figure 6.1: Proposed Algorithm

Figure 6.2: Initial Model

Solve Finite Element Analysis

During the next step, the mesh is generated and the initial structure is solved using Finite Element Analysis (FEA). Deformations and stresses in the structure are obtained.

Generate Initial Population

Then the initial population is generated. As it was mentioned in Chapter 4, the initial population can be set randomly. In proposed algorithm, the initial population is obtained using ESO algorithm. The individuals belonging to the initial population are found as the steps from the ESO algorithm, where the elements are gradually reduced according to the stress level. The example of the initial population consisting of four individuals is shown in Fig. 6.3.

Figure 6.3: Initial Population

The elements with nodes in which the load is applied or the supports placed are kept during the whole process. The example can be found in Fig. 6.4.

Figure 6.4: Elements Kept

Mapping the Structure

In case of genetic algorithm, each structure has to be written in binary code. The elements which are in the structure are represented by number 1, while the elements which do not belong to the structure are written as 0. The example of a structure placed in the domain of size 4 x 3 consisting of 8 elements is shown in Fig. 6.5. The figure also displays the numbering of rectangular elements and the process of obtaining the binary code for the structure (individual).

The size of the chromosome is $n \times 1$, where n is the number of rectangular elements in the initial domain. In case of the structure in Fig. 6.5, the length of the chromosome is 1 x 12. In certain steps of the algorithm, it is necessary to work with matrix of size 4 x 3 which represents the exact location of the elements. These matrices are required for calculation of Euclidean distance, which is calculated using the function *bwdist* provided by MATLAB.

Figure 6.5: Mapping the Structure

Find Cost for Chromosomes

FEA is solved in each GA iteration. The stresses in the structure are necessary for determination of rate of individual. Chromosomes are evaluated according to the cost function (the lower, the better). To find appropriate cost function was a difficult task.

Concrete has different properties in tension and compression. It was decided to find compression dominant structures. It means that the elements in tension have to be eliminated. The stress level in the structure is measured using criterion σ_e which is written for compression dominant structures in Eq. 5.4. The criterion σ_e is calculated

for each element in the structure. The cost function should reflect the behavior of whole structure, and therefore the cost for each individual is calculated as

$$Cost = \sum_{e=1}^n (\sigma_{max} - \sigma_e), \quad (6.1)$$

where σ_{max} is the maximal criterion σ_e in the structure and σ_e is the criterion for the element and n is the number of elements in the structure. The lower Cost occurs for little difference between σ_{max} and σ_e . Cost is also dependent on the number of elements in the structure. The less elements n the smaller Cost.

Arithmetic Crossover

The selection of the individuals is done using the Rank Selection described in Chapter 4. The selected individuals are mated using arithmetic crossover.

First, the elements of selected individuals are reduced according to the stress level. The elements that satisfy the following condition are removed from the structure. Condition is defined as

$$\frac{\sigma_e}{\sigma_{max}} \leq \frac{P \cdot i}{N}, \quad (6.2)$$

where σ_e is the criterion used for the compression dominant structures given in Eq. 5.4, σ_{max} is maximal criterion σ_e in the structure, i is the iteration, N is the number of iterations and P is the random number that varies within the interval $\langle 0, 0.05 \rangle$, where the value 0.05 was found as the most suitable for the functionality of the proposed algorithm.

Then, the arithmetic crossover is used. The offspring arises from the parent chromosomes using conjunction and disjunction operators as is obvious from Fig. 6.6.

Figure 6.6: Crossover

Mutation

When the offspring are created, the process of mutation takes its part. It was decided to use three different kinds of mutation. The first kind of mutations is a binary mutation (bit inversion) which was explained in Chapter 4. The second and third mutation are based on calculation of Euclidean distance, and the elements with some specified distance are added or reduced. All mutations are ongoing with some probability. The example of binary mutation and the structure extension is illustrated in Fig. 6.7. The offspring remains the same after binary mutation, because the elements selected for the binary mutations consists of the load, and therefore the elements can not be removed. The elements with Euclidean distance equal to 1 are added to the structure.

Figure 6.7: Mutation - Structure Extension

The second example of the binary mutation and the structure reduction is shown in Fig. 6.8. From the figure, it is obvious that the binary mutation took its place. The elements with Euclidean distance equal to 1 are removed.

Figure 6.8: Mutation - Structure Reduction

Removal of Detached Structural Parts

If some element is not connected to the rest of the structure it is deleted from the model. The example of removing unconnected element is illustrated in Fig. 6.9. These cases sometimes occur as a result of binary mutation.

Figure 6.9: Unconnected Elements

Different problem occurs when the structure is disconnected, that means the supports and the loads are not connected through elements. These kinds of inappropriate structures can come from the arithmetic crossover when the large part of the structure is removed due to the stress level. The developed algorithm provides the possibility to extend the disconnected parts in order to connect them together, the process is shown in Fig. 6.10. If the structure is still disconnected after this step, then it is rejected from the calculation. It means that these structures have no chance to go successfully through the selection process.

Figure 6.10: Disconnected Structure

Adding Material

The elements are added to the places with the high stresses. High stress levels are determined according to the yield surface in the principal plane stress space shown in Fig. 6.11. The elements are added around the area where the stress does not meet the condition. According to the CEB-FIP Model Code 90, the strength of concrete under biaxial states of stress is expressed using the conditions shown in Tab. 6.1.

Table 6.1: CEB-FIB Conditions

Function	Range
$\sigma_2 = -\frac{1+3.8\alpha}{(1+\alpha)^2} f_{uc}$	$\sigma_2 < -0.96 f_{uc}$
$\sigma_1 = \left(1 + 0.8 \frac{\sigma_2}{f_{uc}}\right) f_{ut}$	$-0.96 f_{uc} \leq \sigma_2 < 0$
$\sigma_1 = f_{ut}$	$\sigma_2 \geq 0$

The input parameters for the strength of concrete under biaxial states of stress determining are the strengths in uniaxial compression f_{uc} and in uniaxial tension f_{ut} , [5]. The parameter α is calculated as ratio σ_1/σ_2 , while $\sigma_1 \geq \sigma_2$ is assumed. The biaxial compressive strength f_{2uc} is assumed $1.2f_{uc}$. The example of biaxial strength of concrete is shown in Fig. 6.11.

Figure 6.11: Biaxial Strength of Concrete

The principle of adding material is shown in Fig. 6.12, where the material is added to the places with euclidean distance less than two. In the proposed algorithm, the material is added to the places with euclidean distance set according to the size of finite elements. For elements of the size 0.1 x 0.1 m is the distance less than or equal to two.

Figure 6.12: Adding Material

Chapter 7

Examples of Optimized Structures

The structures optimized using the program introduced in Chapter 6 are shown in this chapter. Three examples were chosen to illustrate the process of the optimization using GA.

7.1 Structure 1

As a first example, the structure of size 6 x 9 m ($B \times H$) and the thickness 0.2 m was chosen. The distributed load f equal to 30 kN/m is acting on the top of the structure and in 3 and 6 m. The structure has fixed supports on the bottom edge as is shown in Fig. 7.1, each support is 0.2 m wide. The structure is solved as symmetric, whole structure is divided into 5400 elements of size 0.1 x 0.1 m. The initial population is made using the ESO algorithm, RR_0 and ER are set to 0.1 %. All the input parameters are shown in Table 7.1.

Figure 7.1: Structure 1 - Design Domain

The structure was optimized using program described in previous chapter. The whole calculation took 152 minutes. In each generation, 20 different structures were solved, which were each time evaluated using formula in Eq. 6.1. The evolution of cost is shown in Fig. 7.2, where the left graph shows evolution of best cost during generations, while

the right graph shows the evolution of average cost during generation. It is obvious that the curve is decreasing which means the structures are improving.

Table 7.1: Structure 1 - Input Parameters

Structure	
Size B x H	6 x 9 m
Thickness	0.2 m
Initial number of elements	5400
Mesh size	0.1 x 0.1 m
Material Parameters	
Modulus of elasticity E	33 GPa
Poisson's ratio ν	0.2
Concrete density ρ_c	2500 kg/m ³
Strength in compression f_{cu}	20 MPa
Strength in tension f_{tu}	2 MPa
Load	
Distributed load f	30 kN/m
Gravity constant g	10 m/s ²
GA Parameters	
Number of chromosomes	20
Number of generations	50
Mutation probability	1 %
Elitism	10 %

Figure 7.2: Structure 1 - The Evolution of Cost

Figure 7.3: Structure 1 - Distribution of Principal Stress σ_1

During the process, the structure with the lowest cost was saved in each generation. As a result, 50 various structures are obtained. Structures can be used as an inspiration for the design. For the illustration, 12 structures were chosen and the principal stresses σ_1 and σ_2 are compared. These structures are shown in Fig. 7.3 and 7.4. The structure from generation 47 has the lowest cost, this structure is considered as a resulting structure of GA. It is compared with the initial structure of GA in Table 7.2. The maximal principal stress $\sigma_{1,max}$ of a resulting structure is a bit higher than the concrete strength in tension. It is assumed that the reinforcement would be in final design included.

Table 7.2: Structure 1 - Results

	Initial structure (Generation 1)	Best rated structure (Generation 47)
$\sigma_{1,max}$ [MPa]	0.3	2.5
$\sigma_{2,min}$ [MPa]	-10.1	-7.4
$Cost$ [MPa]	27205	4493
Number of elements n	5112	1616

Figure 7.4: Structure 1 - Distribution of Principal Stress σ_2

The principal stresses and the deformed shape of the best rated structure are shown in the Fig. 7.5. The global deformation u is calculated as $\sqrt{u_x^2 + u_y^2}$. In the figure, the factor of deformations equal to 1000 is used.

Figure 7.5: Structure 1 - The Best Rated Structure

Comparison of Results

It must be always kept in mind that the results are influenced by the random operations of GA. It is recommended to run the calculation at least twice to make sure the results are appropriate.

Figure 7.6: Structure 1 - The Evolution of Cost, 2nd Calculation

Figure 7.7: Structure 1 - Distribution of Principal Stress σ_1 , 2nd Calculation

Therefore the first example was calculated twice and the result of the second calculation are shown here. The evolution of cost for the second calculation of GA is shown in Fig. 7.6. The Fig. 7.7 shows the structures and the principal stress distribution during the steps of GA. Comparison of the first and the second calculation is shown in Table 7.3.

Table 7.3: Structure 1 - Comparison of Calculations

	1st Calculation	2nd Calculation
Elapsed Time [min]	152	150
Best Rated Structure	Generation 47	Generation 48
$\sigma_{1,max}$ [MPa]	2.5	5.4
$\sigma_{2,min}$ [MPa]	-7.4	-7.7
<i>Cost</i> [MPa]	4493	4700
Number of elements n	1616	1646

7.2 Structure 2

As a second example, the structure of size 6 x 6 m ($B \times H$) and the thickness 0.2 m was chosen. The distributed load f equal to 30 kN/m is acting on the top of the structure and in 3 m. The structure has fixed supports on the bottom edge as is shown in Fig. 7.8, each support is 0.2 m wide. The structure is solved as symmetric, whole structure is divided into 3600 elements of size 0.1 x 0.1 m. The initial population is made using the ESO algorithm, RR_0 and ER are set to 0.1 %. All the input parameters are shown in Table 7.4.

Figure 7.8: Structure 2 - Design Domain

The structure was optimized using program described in previous chapter. The whole calculation took 111 minutes. In each generation, 20 different structures were solved. The structures were evaluated using formula in Eq. 6.1.

Figure 7.9: Structure 2 - The Evolution of Cost

The evolution of cost shows Fig. 7.9, where the left graph shows evolution of best

cost during generations, while the right graph shows the evolution of average cost during generation. It is obvious that the curve is decreasing which means the structures are improving.

Table 7.4: Structure 2 - Input Parameters

Structure	
Size B x H	6 x 6 m
Thickness	0.2 m
Initial number of elements	3600
Mesh size	0.1 x 0.1 m
Material Parameters	
Modulus of elasticity E	33 GPa
Poisson's ratio ν	0.2
Concrete density ρ_c	2500 kg/m ³
Strength in compression f_{cu}	20 MPa
Strength in tension f_{tu}	2 MPa
Load	
Distributed load f	30 kN/m
Node load F	20 kN
Gravity constant g	10 m/s ²
GA Parameters	
Number of chromosomes	20
Number of generations	100
Mutation probability	1 %
Elitism	10 %

Figure 7.10: Structure 2 - Distribution of Principal Stress σ_1

During the process, the structure with the lowest cost was saved in each generation. As a result, 100 various structures are obtained. Structures can be used as an inspiration for the design. For the illustration, 12 structures were chosen and the principal stresses σ_1 and σ_2 are compared. These structures are shown in Fig. 7.10 and 7.11. The structure from generation 97 has the lowest cost, this structure is considered as a resulting structure of the GA. It is compared with the initial structure of GA in Table 7.5. The maximal principal stress $\sigma_{1,max}$ of a resulting structure is a bit higher than the concrete strength in tension. It is assumed that the reinforcement would be in final design included.

Table 7.5: Structure 2 - Results

	Initial structure (Generation 1)	Best rated structure (Generation 98)
$\sigma_{1,max}$ [MPa]	0.3	2.9
$\sigma_{2,min}$ [MPa]	-7.7	-6.9
<i>Cost</i> [MPa]	2615	13226
Number of elements n	3292	1160

Figure 7.11: Structure 2 - Distribution of Principal Stress σ_2

The principal stresses and the deformed shape of the best rated structure are shown in the Fig. 7.12. The global deformation u is calculated as $\sqrt{u_x^2 + u_y^2}$. In the figure, the factor of deformations equal to 1000 is used.

Figure 7.12: Structure 2 - The Best Rated Structure

Comparison to ESO

The results were compared to the structures optimized using ESO described in Chapter 5. The material is removed based on the stress level that is measured using criterion σ_e defined in Eq. 5.4. The parameters of ESO RR_0 and ER are set to 0.5 %. The 200 iterations were calculated in elapsed time 12 minutes. The twelve structures obtained during the ESO algorithm are shown in Fig. 7.13. The figure can be compared to the Fig. 7.11.

Figure 7.13: Structure 2 - Distribution of Principal Stress σ_2 , ESO

7.3 Structure 3

As a third example, the structure of size 12 x 6 m ($B \times H$) and the thickness 0.2 m was chosen. The distributed load f equal to 30 kN/m is acting on the top of the structure and in 3 m. The structure has fixed supports on the bottom edge as is shown in Fig. 7.14, each support is 0.2 m wide. The structure is solved as symmetric, whole structure is divided into 7200 elements of size 0.1 x 0.1 m. The initial population is made using the ESO algorithm, RR_0 and ER are set to 0.1 %. All the input parameters are shown in Table 7.6.

Figure 7.14: Structure 3 - Design Domain

The structure was optimized using the algorithm described in previous chapter. The whole calculation took 630 minutes. In each generation, 20 different structures were solved. The structures were each time evaluated using formula in Eq. 6.1.

Figure 7.15: Structure 3 - The Evolution of Cost

The evolution of cost is shown in Fig. 7.2, where the left graph shows evolution of best cost during generations, while the right graph shows the evolution of average cost during generation. It is obvious that the curve is decreasing which means the structures are improving.

Table 7.6: Structure 3 - Input Parameters

Structure	
Size B x H	12 x 6 m
Thickness	0.2 m
Initial number of elements	7200
Mesh size	0.1 x 0.1 m
Material Parameters	
Modulus of elasticity E	33 GPa
Poisson's ratio ν	0.2
Concrete density ρ_c	2500 kg/m ³
Strength in compression f_{cu}	30 MPa
Strength in tension f_{tu}	3 MPa
Load	
Distributed load f	30 kN/m
Node load F	50 kN
Gravity constant g	10 m/s ²
GA Parameters	
Number of chromosomes	20
Number of generations	100
Mutation probability	1 %
Elitism	10 %

Table 7.7: Structure 3 - Results

	Initial structure (Generation 1)	Best rated structure (Generation 76)
$\sigma_{1,max}$ [MPa]	0.6	2.6
$\sigma_{2,min}$ [MPa]	-7.4	-6.1
$Cost$ [MPa]	25804	6151
Number of elements n	6642	2514

Figure 7.16: Structure 3 - Distribution of Principal Stress σ_1

Figure 7.17: Structure 3 - Distribution of Principal Stress σ_2

During the process, the structure with the lowest cost was saved in each generation. As a result, 100 various structures are obtained. Structures can be used as inspiration for the design. For the illustration, 12 structures were chosen and the principal stresses σ_1 and σ_2 are compared. These structures are shown in Fig. 7.16 and 7.17. The structure from generation 76 has the lowest cost, this structure is considered as a resulting structure of GA. It is compared with the initial structure of GA in Table 7.7.

The principal stresses and the deformed shape of the best rated structure are shown in the Fig. 7.18. The global deformation u is calculated as $\sqrt{u_x^2 + u_y^2}$. In the figure, the factor of deformations equal to 1000 is used.

Figure 7.18: Structure 3 - The Best Rated Structure

Architectural Aspects

The previous structures can be used as an inspiration for the next design. However, it is necessary to modify the resulting structure to be able to use it for the design. The example of modified structure is shown in the following Fig. 7.19.

Figure 7.19: Structure 3 - Resulting Structure

The structure differs in shape, that is why the stress analysis has to be calculated again. It was decided to use FEA program RFEM for determining the deformations and stresses. This calculation is also a little verification of the results obtained from the developed program in MATLAB. The distribution of the principal stresses and the deformations are shown in Appendix. The structure from Fig. 7.19 is used in the following visualization.

Figure 7.20: Structure 3 - Visualization

Chapter 8

Construction Aspects

The resulting structures obtained in the previous chapter are remarkably shaped. The proposed algorithm can find applications in architecture, that the structures obtained in the previous chapter demonstrate. The structures that came from the optimizing process needs to be modified to obtain the shape which is possible to construct. However, the construction of such as complicated structures could be still quite difficult challenge. This fact is proved by the two examples of extraordinary organic shaped structures that are shown in this chapter.

Both structures were designed by architecture studio Kuryłowicz & Associates. The first great example of extraordinary construction is the structure of Prosta Tower situated in Warsaw, Poland. Prosta Tower was constructed between the years 2007 and 2011, while the structural work took only 11 months. The 19 stories building's façade is made of diamond-shaped reinforced concrete sections with perfect architectural concrete finish. The structure is shown in Fig. 8.1.

Figure 8.1: Prosta Tower, [4]

The second example of great work of this studio is definitely Warmińska Shopping Gallery situated in Olsztyn, Poland. The Fig. 8.2 shows the building also during the construction.

Figure 8.2: Warmińska Shopping Gallery, [2], [15]

These examples show that the construction of the unusually shaped structures is possible, but it brings a great challenge during the construction process. It is obvious, that the structures require special formwork and the perfect control of the whole construction process, but the result is worth it.

Chapter 9

Conclusions

In this diploma thesis, a developed algorithm which seeks the optimal shape of concrete structures was introduced.

The algorithm is inspired by Evolutionary Structural Optimization method (ESO) which is based on removing inefficient material from the structure. At first, it was decided to implement the ESO and find out the advantages and disadvantages of this method. This knowledge was used for the implementing the optimizing process. To find out the optimal shape is a great problem, due to this fact, it was decided to use the Genetic Algorithm (GA), which is generally used for finding solutions to complex search problems.

The ESO works fine for the simple structures such as those which were solved in Section 5.1. But for the more complex structures, the algorithm does not fit well. In some step of ESO, a lot of material can be removed and the structure is no longer suitable. This problem can be solved by adding the material to the highly stressed places. It was decided to introduce this feature to the developed algorithm. Therefore in each step, the inefficient material is moved to the surroundings of highly stressed places. The highly stressed places are decided as those, where the biaxial concrete strength is exceeded. The biaxial concrete strength is determined according to the CEB-FIP Model Code 90.

In each step of genetic algorithm, n different structures are calculated. This is the main difference to the ESO. The searching space of GA is larger. It is expected, that the structures which would be probably skipped in the ESO are found and calculated in the developed algorithm. During the process, all the structures are modified, evaluated and combined with hope to find out the remarkably shaped compression dominant structure.

The introduced algorithm was implemented in MATLAB Environment. The Finite Element Method is used for determining the deformations and the stresses distributions in the structure. The rectangular elements with eight degrees of freedom are used. The principal stresses are used for the determination of the utilization of the material in the structure.

Range of Application

It is always important to keep in mind that the results are influenced by randomness which is introduced during genetic algorithm operations. Therefore, the results could differ for the very same input parameters. This behavior of the developed algorithm is proven in Section 7.1, where two runs of the algorithm with same input parameter are compared. It is recommended to run the calculation at least twice to achieve the appropriate results.

The structures are evaluated at each generation of GA. The best evaluated structure does not have to be optimal for the design. Sometimes only the lack of the small number of elements decides the resulting structure. It is recommended to check all the best structures.

The resulting structures can be used as an inspiration for the future design.

Bibliography

- [1] Valério S. Almeida, Hélio Luiz Simonetti, and Luttgardes Oliveira Neto. Comparative analysis of strut-and-tie models using smooth evolutionary structural optimization. *Engineering Structures*, 56:1665 – 1675, 2013.
- [2] Kuryłowicz & Associates. Warmińska Shopping Gallery. <http://www.apaka.com.pl/enhtml/projekty/warminska-shopping-gallery>, Accessed: 2016-11-12.
- [3] C. Cui, H. Ohmori, and M. Sasaki. Computational morphogenesis of 3d structures by extended eso method. *Journal of the International Association for Shell and Spatial Structures*, 44(141):51–61, 2003.
- [4] PERI Formwork Scaffolding Engineering. Prosta Tower. <https://www.peri.com/en/projects/skyscrapers-and-towers/prosta-tower.html>, Accessed: 2016-11-12.
- [5] fib Fédération internationale du béton. *CEB-FIP Model Code 1990: Design Code*. Bulletin d'information / Comité Euro-International du Béton ; nos.213/214. T. Telford, 1993.
- [6] J. Fish and T. Belytschko. *A First Course in Finite Elements*. Wiley, 2007.
- [7] D. Floreano and C. Mattiussi. *Bio-Inspired Artificial Intelligence: Theories, Methods, and Technologies*. MIT Press, 2008.
- [8] J. Hynek. *Genetic Algorithms and Genetic Programming*. Grada, 2008. in Czech.
- [9] P.I. Kattan. *MATLAB Guide to Finite Elements: An Interactive Approach*. Springer-Verlag Berlin Heidelberg, 2008.
- [10] Hyo-Gyoung Kwak and Sang-Hoon Noh. Determination of strut-and-tie models using evolutionary structural optimization. *Engineering Structures*, 28(10):1440 – 1449, 2006.
- [11] G.R. Liu and S.S. Quek. *The Finite Element Method: A Practical Course*. Elsevier Science, 2003.
- [12] D. Logan. *A First Course in the Finite Element Method*. Cengage Learning, 2012.

- [13] O.M. Querin, V. Young, G.P. Steven, and Y.M. Xie. Computational efficiency and validation of bi-directional evolutionary structural optimisation. *Computer Methods in Applied Mechanics and Engineering*, 189(2):559 – 573, 2000.
- [14] S.S. Rao. *The Finite Element Method in Engineering*. Elsevier Inc., 2011.
- [15] ULMA Construcccion Polska S.A. Galeria Warmińska, Olsztyn, Polska. <http://www.ulmaconstruction.pl/pl/realizacje/centra-handlowe/warminska-olsztyn-polska>, Accessed: 2016-11-12.
- [16] S.N. Sivanandam and S.N. Deepa. *Introduction to Genetic Algorithms*. Springer Berlin Heidelberg, 2007.
- [17] J. W. Tang. Developing evolutionary structural optimization techniques for civil engineering applications. Phd thesis, RMIT University, Australia, 2011.
- [18] D. Veenendaal. Evolutionary optimization of fabric formed structural elements. Masters thesis, Delft University of Technology, the Netherlands, 2008.
- [19] Y.M. Xie and G.P. Steven. *Evolutionary Structural Optimization*. Springer London, 2012.
- [20] Y.M. Xie, Z.H. Zuo, X. Huang, J.W. Tang, B. Zhao and P. Felicetti. Architecture and urban design through evolutionary structural optimisation algorithms. *Keynote Lecture of International Symposium on Algorithmic Design for Architecture and Urban Design, Tokyo, Japan*, 2011.

Appendix

RFEM Results

The structure from the Fig. 7.19 was also calculated in the finite element analysis program RFEM. The results are presented in this appendix.

Figure A.1: Loads

Figure A.2: FE Mesh

Figure A.3: Global Deformation u

Figure A.4: Principal Stress Trajectories

Figure A.5: Principal Stress σ_1

Figure A.6: Principal Stress σ_2